REVIEW ARTICLE
https://doi.org/10.1038/s41566-021-00881-0

nature photonics

Speed scaling in multiphoton fluorescence microscopy

Jianglai Wu[1,2], Na Ji[1,3,4,5,6] ✉ and Kevin K. Tsia[7,8] ✉

After over 30 years of advances, multiphoton microscopy (MPM) is now instrumental in a wide range of in vivo biological imaging applications. However, it has, until recently, remained not achievable or affordable to meet the unmet need for fast monitoring of biological dynamics and large-scale examination of biological heterogeneity. Only within the past few years have new strategies emerged to empower MPM at a speed that was once inconceivable, notably at kilohertz two-dimensional (2D) frame rate, and 3D rate or beyond. This Review highlights the latest high-speed innovations and discusses the potential of their synergism with other advanced, but less speed-centric MPM toolboxes. Recognizing these prospects and challenges could inspire new approaches for reprioritizing imaging speed in future MPM developments.

Leapfrogging advances in modern light microscopy, especially in the past three decades, have unleashed the power to generate numerous high-definition views of cells, tissues and organisms. Many frontier imaging methods now attain a spatial resolution and image contrast that are undoubtedly beyond the imagination of Robert Hooke, who asserted that 'by the help of Microscopes, there is nothing so small as to escape our inquiry' in his masterpiece *Micrographia* in 1665[1]. However, what often escapes our investigations is not just the 'smallness', but also the fast dynamics of cellular processes, which slip under the radar of existing microscopes. Studying the rapidly evolving behaviour of live cells and tissue in vivo, which holds the key to deciphering how cells maintain (or lose control of) their functions in their native biological context, is especially pertinent. Multiphoton microscopy (MPM) stands out among state-of-the-art light microscopy technologies, primarily because of its unique ability to harness the nonlinear light–matter interaction to generate high-resolution (micrometre or even submicrometre) and optically sectioned images even from deep (few millimetres) and highly scattered tissues (for example, the brain, skin and other organs). This attribute has proven instrumental in a wide range of applications that involve in vivo animal imaging and intact tissue imaging, notably neuroscience, developmental biology and cancer research. Since its first working demonstration in 1990[2], MPM has made remarkable progress in pursuing high spatial resolution in deep tissue. However, development in scaling the temporal resolution of MPM has long been lacking.

The fundamental hurdle to be overcome is rooted in the extremely low probabilities of multiphoton (nonlinear) events (for example, multiphoton absorption), as predicted by Maria Göppert–Mayer in 1931[3]. To generate a plausible multiphoton signal strength (or signal-to-noise ratio, SNR), the excitation light intensity has to be concentrated in space as a focused spot and/or in time as a short pulse (Box 1). This explains why the available MPM platforms largely rely on a laser-scanning imaging strategy, that is, scanning a spatially focused, pulsed laser spot across a plane to produce the axially resolved images. Over the years, laser scanning speeds have progressively improved. However, many of the in vivo biological dynamics known or believed to exist have remained out of reach until recently. Notable examples include the millisecond dynamics of the voltage changes of a neuron membrane, cell trafficking dynamics and the in vivo contractile dynamics of striated muscle sarcomeres. Furthermore, high-speed MPM could also find a new application in high-throughput image-based screening. It is especially valuable for revealing the cellular phenotypes that are uniquely read out by MPM contrasts (for example, lipids, metabolites and other chemical constituents revealed by coherent Raman imaging and cellular/tissue structural anisotropy by second harmonic generation).

Within the past few years, we have witnessed an arsenal of novel high-speed MPM strategies that overcome the speed limitations of classical MPM modalities, especially those that are beginning to enable two-dimensional (2D) full-frame MPM at kilohertz rate or volumetric MPM imaging at video rate (and even beyond). It is thus now more affordable to prioritize imaging speed in MPM design and development. Given this acceleration in developments, this Review aims to review the emerging fast MPM strategies from the past five years, mainly in the context of multiphoton fluorescence imaging because of its triumphant high-speed demonstrations in neurobiology and developmental biology. Identifying their strengths and limitations, we will discuss the key challenges ahead for high-speed MPM to support the continuing exploration of the biological enquiries that were once inconceivable.

State-of-the-art methods for high-speed planar access

Traditional imaging strategies (for example, laser scanning using galvo-mirrors) adopted in MPM (Box 2) face challenges if they are to meet the continuing demand for speed. For example, if we were to adopt the standard raster beam scanning approach to achieve the kilohertz (2D) frame rate in MPM required for recording the fast neuronal voltage dynamics in living brains, a line-scan rate well beyond 1 MHz is required—a speed regime unattainable in any classical laser scanners. Different novel strategies have recently emerged to scale MPM speed (Fig. 1a). Generally, the speed-scaling trend

[1]Department of Physics, University of California, Berkeley, CA, USA. [2]Chinese Institute for Brain Research, Beijing, China. [3]Janelia Research Campus, Howard Hughes Medical Institute, Ashburn, VA, USA. [4]Department of Molecular and Cell Biology, University of California, Berkeley, CA, USA. [5]Helen Wills Neuroscience Institute, University of California, Berkeley, CA, USA. [6]Molecular Biophysics and Integrated Bioimaging Division, Lawrence Berkeley National Laboratory, Berkeley, CA, USA. [7]Department of Electrical and Electronic Engineering, The University of Hong Kong, Hong Kong, China. [8]Advanced Biomedical Instrumentation Centre, Hong Kong Science Park, Shatin, Hong Kong, China. ✉e-mail: jina@berkeley.edu; tsia@hku.hk

Box 1 | Essential ingredients for MPM

Although wide-field MPM is feasible, it is generally favourable to spatially focus the excitation beam (mostly by high-numerical-aperture (NA) optics), as the MPM signal scales supralinearly with the excitation intensity and can thus be enhanced exclusively in the perifocal region. This naturally results in an optical sectioning effect, minimizing tissue photodamage (see figure). On the other hand, temporally concentrating the excitation photon density in a short pulse is particularly advantageous as the MPM signal is known to be enhanced by a factor of $1/(\tau R)^{m-1}$ compared to the continuous wave excitation, where R is the pulse repetition rate, τ is the pulse width and m is the number of photons involved in the process (that is, $m=2$ for two-photon absorption). Thanks to the increasingly mature ultrashort pulsed laser technology, all MPM systems now routinely run on excitation laser pulses with subpicosecond width and a rate of 1–100 MHz, offering an enhancement factor of at least 10^4.

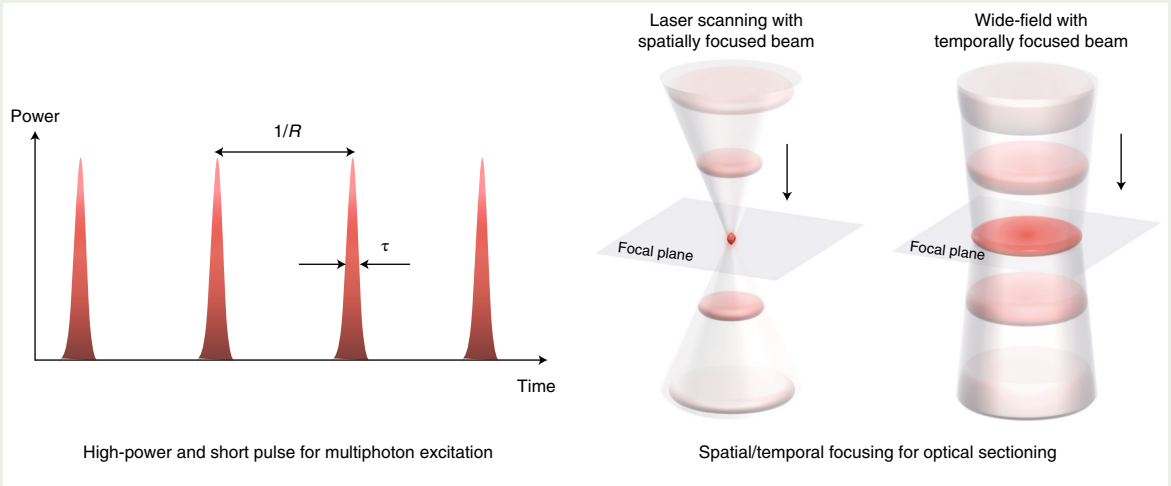

High-power and short pulse for multiphoton excitation

Spatial/temporal focusing for optical sectioning

in the past five years does not scale only in the imaging frame rate (beyond kilohertz), but also in the overall imaging throughput in terms of the image pixel rate (beyond tens of megapixels per second, or even hundreds of megapixels per second). As we will discuss in the following, this substantial progress is made possible with new methods that share similar design rationales: (1) parallelization of sample illumination (with multiple scanning foci, a scanning line beam or even wide-field illumination), (2) multiplexing of image acquisition spatiotemporally, as far as the available photon budget allows (Fig. 2 and Table 1), and (3) a combination of these methods with advanced strategies for enhancing the imaging field of view (FOV; discussed in the section 'Challenges and opportunities ahead').

Kilohertz full-frame 2D MPM with spatiotemporal multiplexing. MPM based on spatiotemporal multiplexing typically scans multiple foci across the sample and records the image signals from these foci simultaneously using a fast detector array/camera or sequentially by a high-speed single-pixel detector. The general rule of thumb is that the more the scanning foci can be generated, the less the time needed to scan across the FOV (that is, higher frame rate). In principle, an array of tens to hundreds of beamlets (in 1D or 2D) can be generated with minimal pulse broadening from an ultrafast laser beam by off-the-shelf optical devices, namely a microlens array (MLA)[4,5], diffractive optical elements[6] and a spatial light modulator (SLM)[7]. In practice, the overall frame rate of multifocal MPM is also influenced by the speed (and sensitivity) of the photodetectors and the scanning speed of the beamlets. Using a state-of-the-art high-speed scientific complementary metal oxide semiconductor (sCMOS) camera and careful design of the MLA-generated beamlet scanning pattern, Zhang et al. recently achieved multifocal (20 × 20) two-photon fluorescence microscopy (2PFM) at 1,000 f.p.s., which revealed fast microcirculation and calcium (Ca^{2+}) dynamics in awake mice brain at millisecond resolution (Fig. 2a)[5]. A major limitation of this method is the background arising from the scattered fluorescence photons in tissue, which thus degrades the image brightness and contrast when imaging deeper.

Instead of using a detector array or camera, multifocal MPM signals can be acquired with a single-pixel photodetector sequentially at high speed by temporally multiplexing the scanning foci. This can be done by introducing a time delay between the scanning foci, either passively or actively. A new technique, called free-space angular-chirp-enhanced delay (FACED), employs a pair of passive (static) and almost parallel mirrors (similar to the concept of an 'infinity mirror') to transform a line-focused pulsed laser beam into a reconfigurable array of spatiotemporally multiplexed beamlets (~100 in practice) and achieved a line-scan rate as high as tens of megahertz (determined by the laser's repetition rate; Fig. 2b). By adding a galvo-mirror (1.5 kHz) to scan the linear array of foci along the slow axis, this technique achieved 2D full-frame 2PFM imaging up to 3,000 f.p.s., capturing the millisecond dynamics of the neuronal voltage events at subcellular resolution in the deep mouse brain (345 μm below the brain surface)[8]. Note that this technique, when applied to fluorescence microscopy, should configure the delay between neighbouring foci longer than the fluorescence lifetime to minimize the crosstalk between the foci. When applied to microscopy utilizing instantaneous coherent light scattering as a contrast mechanism, the delay is only limited by the response time of the photodetector[9]. Another similar approach of spatiotemporal multiplexing is based on spectro-temporal encoding of the scanning foci. This is achieved by active intensity-modulation of a wavelength-swept source to generate a spectrally encoded picosecond (~65 ps) pulse train, then the pulses are sequentially mapped into a linear array of foci on the image plane by a diffraction grating at a line-scan rate of 342 kHz (Fig. 2c)[10]. Although this technique has lower two-photon excitation efficiency because

Box 2 | Traditional strategies for speed scaling in MPM

A classical approach for speeding up MPM imaging is to increase the scanning speed of the spatially focused spot (mostly in a raster-scan manner), as far as the laser scanner design and photon budget allow. The gold-standard laser scanner used in classical MPM is a galvanometric mirror (or galvo-mirror), which currently can achieve a line-scan rate of up to ~10 kHz (panel a in the figure)[129]. Further speed improvement could be achieved by a rotating polygonal mirror, which can scale the speed up to ~100 kHz (panel b in the figure). Combining two galvo-mirrors mirrors (one resonant galvo and one conventional galvo) scanning orthogonally to each other, one could support bioimaging at a 2D video rate, typically 10–30 frames per second (f.p.s.). For a typical image size of 512 × 512 pixels, the frame rate of 30 f.p.s. results in a total pixel rate of ~8 Mpixel s^{-1}. This generally explains that the pixel rate of many conventional MPM systems based on galvo-mirror scanning (most prevalent in the first two decades after the first MPM system was invented in the early 1990s) is well below 10 Mpixel s^{-1} (see the speed-scaling progress plot in Fig. 1a). Although the speed of the galvo-mirror is fundamentally limited by mechanical inertia, there is a family of non-mechanical (inertia-free) laser scanners, including acousto-optic deflectors (AODs) and electro-optic deflectors (EODs), that allow faster scanning at up to hundreds of kilohertz, albeit compromising the angular scan range, number of resolvable scan points and thus the imaging FOV[130].

To achieve volumetric MPM, the most common approach is to translate the imaging objective lens axially using a mechanical actuator (for example, a piezoelectric scanner) and to perform planar image acquisition at each axial step (panel c in the figure). In general, due to the mechanical inertia of the bulk objective, 3D MPM based on axial objective scanning is limited to a volume rate of 1–10 Hz, with a limited number of image planes[131], except with a 'roller-coaster' scanning strategy that compromises the scan depth (for example, 28 µm at 150 Hz and 17 µm at 700 Hz)[132].

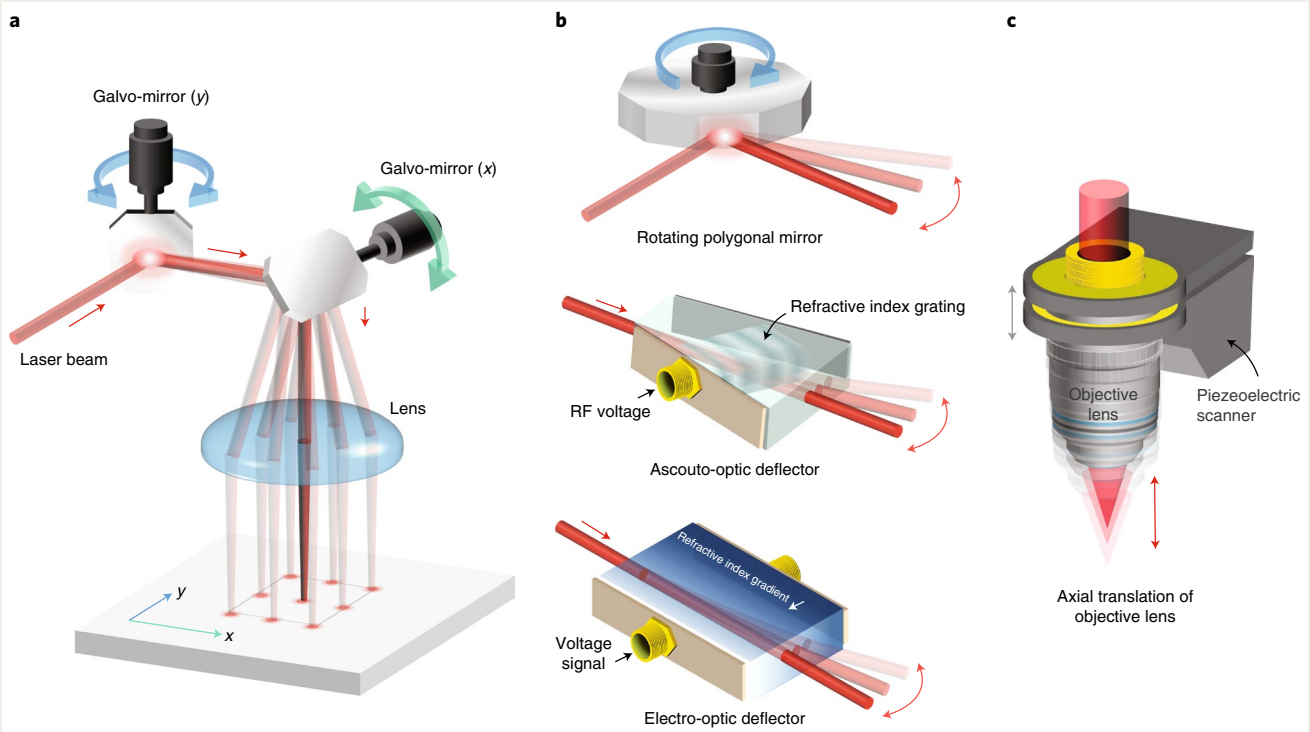

of the longer pulses, it allows 2PFM and two-photon fluorescence lifetime imaging microscopy (2P-FLIM) of microalgae at a 2D frame rate of 2,000 f.p.s. (or at a throughput of 10,000 cells per second). One should note that pixel binning is necessary to yield enough photon budget for high-fidelity lifetime extraction at this speed. It thus compromises the spatial resolution in high-speed 2P-FLIM.

Subkilohertz wide-field MPM in 2D. Instead of using a scanning array of discrete foci, high-speed parallelized acquisition can, in principle, be realized by continuous wide-field illumination in 1D or 2D. In this scenario, the imaging speed is largely governed by the frame rate of the camera, which has been progressively accelerated over the years. Despite state-of-the-art high-speed cameras (for example, a sCMOS camera and a gated intensified camera[11,12]) now enabling sensitive wide-field fluorescence imaging at a 2D frame rate beyond 1,000 f.p.s. at high resolution (>1,000 × 1,000 pixels), wide-field MPM faces two critical challenges to achieve a kilohertz frame rate. First, widespread illumination across a large area significantly reduces the excitation intensity and thus imaging sensitivity. Second, wide-field multiphoton detection degrades the image quality with increasing imaging depth because of signal contamination by scattered fluorescence photons. Among the available wide-field approaches, temporal focusing (TF)[13] and light-sheet illumination[14] (also called selective plane illumination microscopy, SPIM) stand out in pushing the speed limit of wide-field MPM.

TF is a 'light sculpting' technique in which multiphoton absorption is reinforced in the focal plane and rapidly diminished away from it, resulting in optical sectioning even if the illumination is spatially weakly focused[15–17] (Fig. 2d). To obtain sufficient excitation

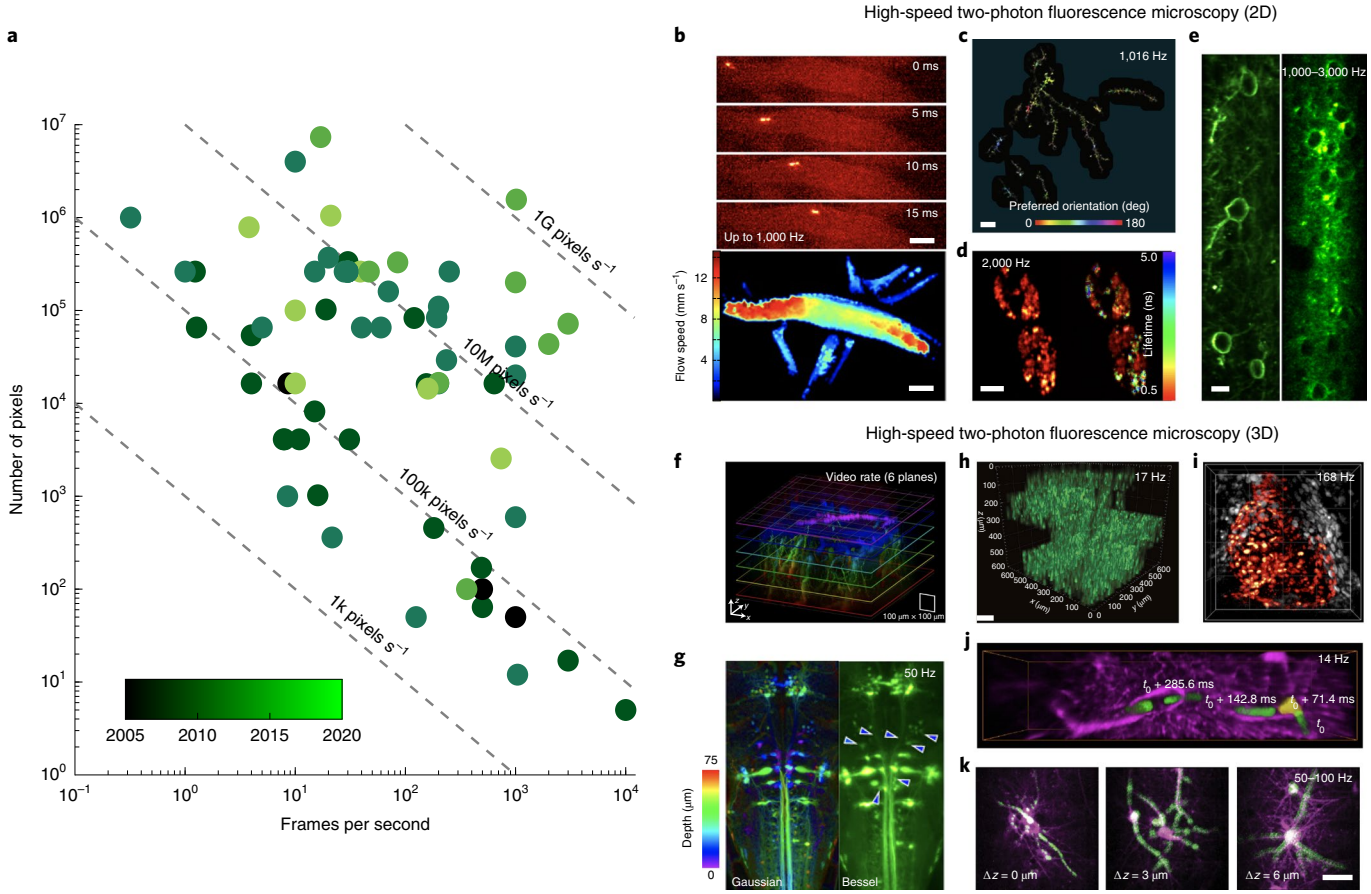

Fig. 1 | Advances in high-speed 2PFM. a, 2PFM imaging throughput scaling from 2005 to 2020 (Supplementary Table). **b**–**k**, Recent 2PFM demonstrations with kilohertz 2D frame rate (**b**–**e**) and >10-Hz volumetric (3D) frame rate (**f**–**k**). **b**, Flowing HEK-293T cells (top images) and the flow speed map in cerebral arterioles (bottom). **c**, Glutamate activity in mouse cortical dendrites. **d**, 2PFM (left) and 2P-FLIM of *Euglena gracilis* (right). **e**, Kilohertz voltage imaging in awake mouse brain. **f**, Multiplane 2PFM of mouse brain vasculature. **g**, Projected 2PFM of reticulospinal and vestibulospinal neurons in a larval zebrafish by Gaussian (left) or Bessel (right) beam scanning. Arrowheads (same colour code as in the depth colour bar) point to example structures (neurons or axons) at a deeper depth. **h**, Large-area 3D Ca^{2+} recording in mouse posterior parietal cortex. **i**, 3D imaging of zebrafish heart beating. **j**, Neutrophil trafficking in mouse cerebral cortex. **k**, Ca^{2+} dynamics (green) of cultured neurons at different depths overlaid with structural images (magenta). Scale bars, 10 μm (**b**–**e**) and 50 μm (**k**). Images reproduced with permission from: **b**, ref. [5], Springer Nature America, Inc.; **c**, ref. [27], Springer Nature America, Inc.; **d**, ref. [10], under a Creative Commons license CC BY 4.0; **e**, ref. [8], Springer Nature America, Inc.; **f**, ref. [54], Nature America, Inc.; **g**, ref. [57], OSA; **h**, ref. [74], Elsevier; **i**, ref. [24], OSA; **j**, ref. [40], Springer Nature America, Inc.; **k**, ref. [20], OSA.

efficiency, wide-field TF MPM commonly employs high-energy (on the scale of microjoules per pulse) short-pulsed lasers (sub-picosecond) with low repetition rate (submegahertz) to boost the multiphoton excitation enhancement factor $1/(\tau R)^{m-1}$ (Box 1). A wide-field (diameter of 60 μm) TF 2PFM system has achieved Ca^{2+} imaging of GCaMP5 in the head of *Caenorhabditis elegans* at a 2D frame rate up to 200 f.p.s. (ref. [13]). Special care should be taken to ensure that the overall average power and thus thermal load deposited on the biological samples are kept low to minimize the risk of photoperturbation and photodamage[18]. To ensure sufficient SNR and minimize the thermal load at high speed, one could also carefully restrict the FOV of interest and reduce the parallelization to 1D line-scanning, which appears to be more practically scalable in the TF-based MFM speed[19,20].

Light-sheet imaging or SPIM is another promising parallelized imaging strategy that offers tremendous promise in fluorescence imaging at high speed and with low phototoxicity (Fig. 2e)[21]. Similar to the case of wide-field TF, parallelization in two-photon SPIM is preferably implemented in a 1D line-scanning mode (that is, scanning of the illumination beam synchronously with the camera readout) to attain sufficient SNR[14,22–24] at high speed, for example, in vivo two-photon SPIM of the zebrafish heart at 488 f.p.s. (ref. [24]). One technical restriction of SPIM is that the orthogonality between the illumination and detection paths generally requires a dual-objective geometry and thus generally limits its applications to biological samples (for example, zebrafish larvae and *Drosophila*) that can be easily immobilized and accessed from different orientations. Different implementations of single-objective SPIM, which are generally compatible with MPM, have recently been developed and show initial promise to address this optical access issue without compromising speed[12,25,26].

Kilohertz computational MPM in 2D. Recently, a tomographic imaging strategy also showed initial promise in achieving a kilohertz frame rate[27]. This method applies sequential line-scanning traversing the FOV along four different directions (or projections) and compresses all the pixels along the line-scan into a single measurement by a detector (Fig. 2f). By leveraging the prior morphological information of the sample (the brain structural image at dendritic resolution) pre-captured using slow raster scanning, one can reconstruct the fast dendritic glutamate transients across the FOV from the four projections continuously recorded

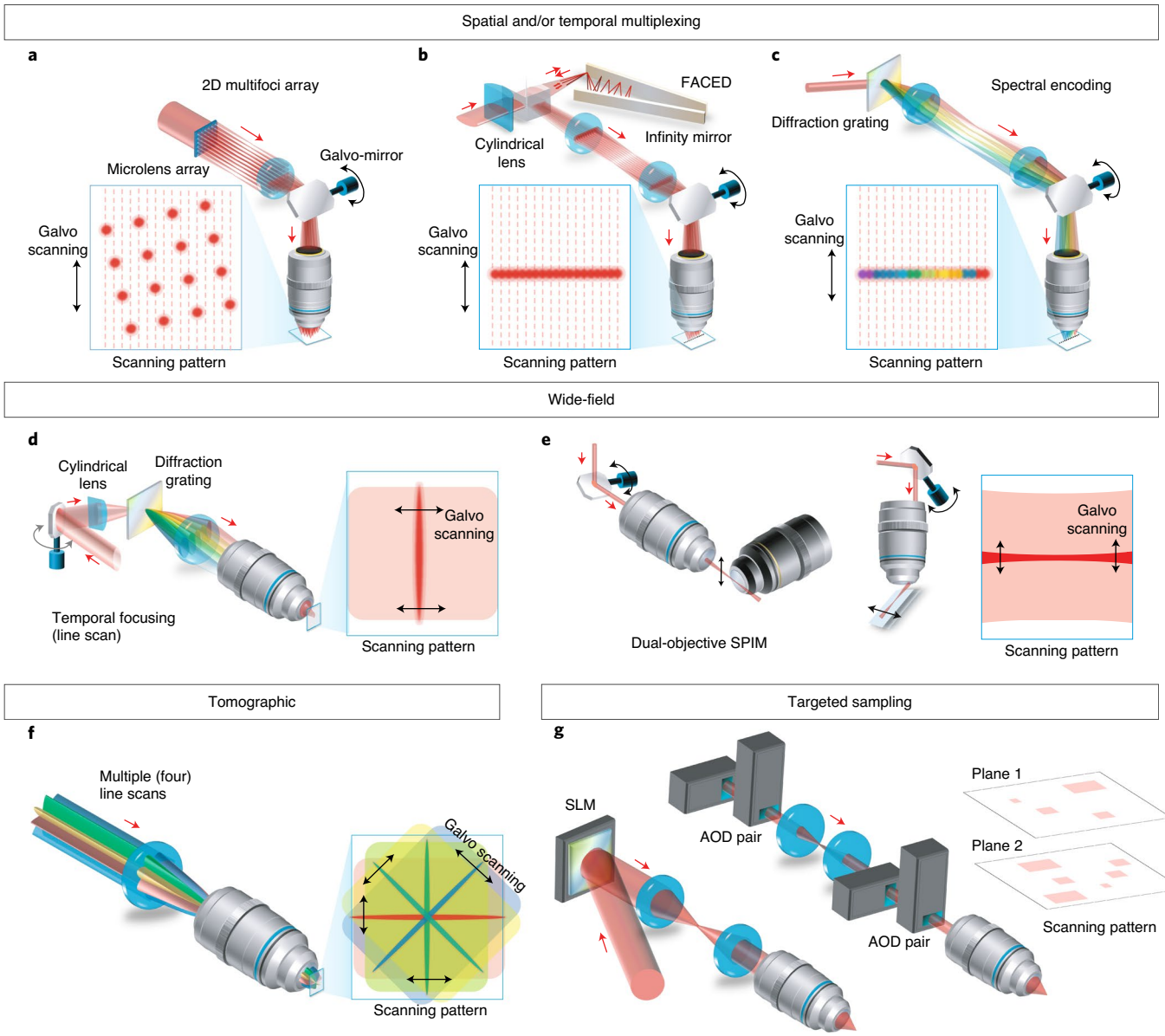

Fig. 2 | High-speed strategies enabling planar MPM at subkilohertz to kilohertz frame rate. a, Generation of a 2D multifoci array (for example, 20 × 20) combined with linear scanning of the array at a tilt angle. **b**, FACED: generation of a linear array of foci by an infinity mirror. **c**, Generation of a linear array of spectrally encoded foci based on the use of a diffraction grating and a high-speed wavelength-swept source. **d**, Temporal focusing for wide-field MPM (in 1D). **e**, Wide-field MPM by SPIM using either a dual-objective or single-objective approach. **f**, Tomographic MPM, achieved by sequentially scanning a line beam along four different orientations. **g**, Targeted/on-demand sampling. This accesses multiple areas on the plane at high speed either sequentially by scanning the focus beam using an AOD or simultaneously by holographic projection using an SLM. Note that these targeted sampling methods can also be achieved in 3D, that is, with multiple planes in the axial dimension.

at 1,016 f.p.s. The tomographic approach requires fewer measurements than the compressive-sensing-based wide-field MPM, which requires more measurements for final image reconstruction, and hence is slower[28]. Nevertheless, the image reconstruction accuracy in this tomographic approach requires a lack of axial sample motion. It is subject to stronger prior information of the 'sparseness' for the sample (typically employed in many other compressive-sensing methods) as well as the fluorescence signal dynamics. These priors are particularly applicable to many high-resolution brain-imaging applications where the imaged neurons are sparsely populated and/or the neuronal spiking activities are sparse. An additional SLM masking was also employed to allow dynamical glutamate activity recording within the areas of interest with the user-defined line-scan patterns. Not only can this masking reduce signal mixing and thermal load, but it also artificially introduces sparsity in the densely labelled samples.

Kilohertz targeted sampling. A targeted sampling strategy can be used if prior knowledge of the spatial information of specific structures (for example, neurons or vasculatures) is available. In a usual protocol, these regions are first identified with a prior full-frame scan in 2D or 3D. The laser focus (or foci) is then rapidly moved (hopped), commonly by AOD scanners, to the identified regions of interest in 2D or 3D for MPM excitation and readout (Fig. 2g). This targeted approach is particularly favourable for accelerating the imaging speed (compared to the raster scan) while maximizing the

Table 1 | Representative techniques to scale the MPM speed

Key technique	Working principle	Imaging access	Imaging speed (Hz)	Remarks and caveats	Ref.
Full-frame spatial and/or temporal multiplexing[a]	Multifoci excitation	Planar	1,000 (2D)	1D fast galvo scanning of a tilted array of 2D foci (for example, 20 × 20) generated by an MLA; presence of background fluorescence arising from the scattered fluorescence photons	5
	All-optical laser scanning	Planar	1,000–3,000 (2D)	Fast line-scan rate (>1 MHz) by linear virtual source array generation using an infinity mirror; number of scanning foci (~100) is governed by the infinity-mirror geometry and fluorescence lifetime	8
	Spectro-temporal encoding	Planar	2,000 (2D)	Fast line-scan rate (>1 MHz) using a diffraction grating and fast wavelength-swept source; fluorescence excitation efficiency could be limited by the narrow spectral width of each spectrally resolvable focus	10
Wide-field[b]	Light-sheet illumination	Planar and axial	<500 (2D); 1–10 (3D)[c]	Optical sectioning by orthogonal detection of light-sheet illumination; the line-scanning mode is preferred for sufficient SNR; imaging speed is limited by the frame rate of the 2D image sensor; signal crosstalk due to tissue scattering	14,22–25
	Temporal focusing	Planar	10–100 (2D)[d]	Line-scanning mode is preferred for sufficient SNR; imaging speed is limited by the frame rate of the 2D image sensor; special care is needed to minimize the thermal load due to wide-field excitation; signal crosstalk due to tissue scattering	13,19
Line-scan tomography	Scanned-line angular projection	Planar	1,000 (2D)	High-speed sequential line-scanning along multiple projections; single-pixel detection of all line scans; additional computation cost for image reconstruction; prior knowledge of sample structure is required	27
Target sampling[e]	Random access	Planar and axial	1,000s (2D); 10–100 (3D)	Mainly based on an AOD; imaging speed inversely scales with the number of targeted points or effective FOV in 2D/3D; prior knowledge of the sample is required; susceptible to motion artefacts	29–35
Fast axial scanning	Inertia-free axial focus shift	Axial	<100 (3D)	Axial scan speed: ~1 kHz (electrically tunable lens) and up to 1 MHz (TAG lens); extra optical aberration introduced	39–41
	Remote focusing	Axial		Axial scanning at ~ 1 kHz with minimal optical aberration; extra relay optics required	45–49,74,86
Multiplane imaging	Axial spatiotemporal multiplexing	Axial	30–60 (3D)	Nearly simultaneous multiplane imaging at different depths; typically limited to a few planes (2–6 planes) depending on the laser's repetition rate and fluorescence lifetime	51,54,74
Extending the depth of field	PSF engineering	Axial	10–100 (2.5D)[f]	Using elongated PSF (Bessel, Airy and V-shaped foci) to project a 3D image onto a 2D plane; effectively transfer the 2D frame rate to the volume rate; tailored for sparsely expressed samples; axial resolution compromised	56–61,73,88,89,94

[a]Full-frame refers to the full scanning coverage accomplished by the technique. [b]Wide-field 2PFM refers to two-photon excitation with continuous wide-field (line or plane) illumination instead of discrete-foci illumination (for example, the techniques based on spatial/temporal multiplexing or targeted sampling). Both wide-field and discrete-foci illumination methods allow full-frame imaging. [c]A time synchronization algorithm can be used to achieve an equivalent 3D frame rate as high as 168 Hz (ref. [24]). [d]Temporal focusing can also be used to engineer the shape of the scanning focus (not necessarily diffraction-limited) for a raster scan[74]. [e]The reported imaging speed of target sampling is not often equivalent to the full-frame rate. Instead, it is the speed required to image one or multiple regions of interest (of any arbitrary shape), which is not the entire full-frame region. [f]2D projection of a 3D volume.

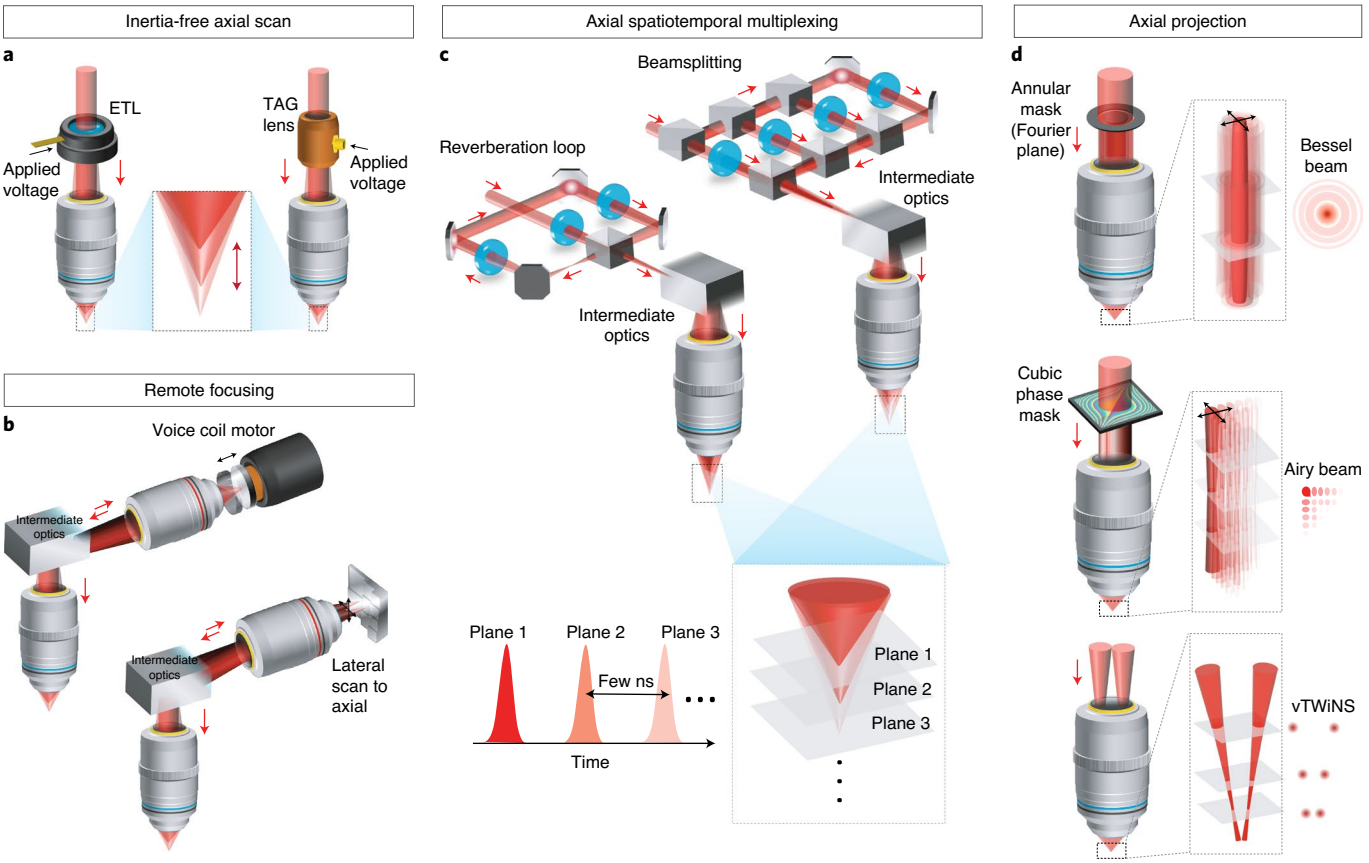

Fig. 3 | Strategies for high-speed MPM axial access. a, Inertia-free axial scan by an ETL or TAG lens, which controls the beam divergence and thus the focal plane. **b**, Remote focusing by an objective and an axially scanned mirror (actuated by a voice coil motor) positioned at the conjugate plane of the sample. This can also be done by transforming lateral beam scanning across a remote step-mirror into an axial focal shift. **c**, Axial spatiotemporal multiplexing by splitting the excitation pulses into multiple time-delayed beamlets focused onto different depths. This is accomplished by multiple optical delay lines or a reverberation optical loop. **d**, Axial projection by an axially elongated scanning focus (for example, a Bessel beam generated by an annulus mask (or using an axicon or SLM) and an Airy beam generated by a cubic phase mask). One can also scan a stereoscopic V-shaped beam to generate twin 2D projection images that encode the axial information.

SNR and minimizing the thermal load and phototoxicity. There is a major class of high-speed in vivo Ca^{2+} imaging techniques, called random-access microscopy, that exploits the fast foci scanning and switching stability of AODs[29,30]. Advanced random-access MPM can scale up the Ca^{2+} imaging speed to the kilohertz regime by carrying out various fast user-defined scanning strategies, such as targeted multiple subvolume, plane, line and point scanning, with a focus jumping time on the order of microseconds and a line-scan rate of up to 100 kHz (refs. [31,32]). In general, there is a trade-off between the speed and the number of targeted regions (for example, neurons) that can be imaged (for example, Ca^{2+} transient recording of 5–30 neurons at a speed of ~1 kHz versus tens to hundreds of neurons at a lower rate of 0.1–0.2 Hz; refs. [31,32]). Taking advantage of new voltage indicator development, high-speed random access MPM has also enabled direct recording of action potentials[33–35]. It has been used for tracking voltage spikes (for example, 25 scan points on the dendritic tree[34]) in organotypic brain slice cultures as well as in the cortical and hippocampal neurons of awake behaving mice at a sampling rate of 15 kHz per neuron[35]. The random-access sampling strategy also can be adopted in digital micromirror device-based 2PFM to achieve focus scanning and switching up to 22.7 kHz (ref. [36]). Apart from accessing multiple points in a sequence, an SLM can be used to generate multiple random-access foci in parallel and to adopt wide-field detection to allow imaging at high speed[20]. A balance among the number of targeted points, the excitation efficiency and possible signal crosstalk due to tissue scattering is necessary during experimental design. Random-access sampling is susceptible to sample movements and can result in motion artefacts that cannot be easily corrected post hoc, especially when imaging awake behaving animals. Variants of random-access 2PFM involving driving the AODs to quickly scan a local volume surrounding the targeted points can minimize such motion artefacts[32,35]. Recently, a real-time motion correction approach has been developed to track brain movements at 1 kHz and correct motion artefacts at submicrometre precision in behaving animals[37].

State-of-the-art methods for high-speed axial access

To maintain a similar level of SNR and thermal load as 2D MPM, volumetric MPM generally requires some degree of sequential acquisition instead of full 3D parallelization, that is, scanning the laser focus, foci or 1D/2D wide-field illumination beam/sheet in the axial direction (Table 1). Hence, the overall volumetric rate has to be scaled down. Because of the diverse methods for accessing image information in 3D, the reported volumetric imaging rates in the literature should be interpreted carefully. There are three major strategies for volumetric MPM: (1) continuous volumetric sampling, (2) discrete multiplane sampling and (3) projection sampling by extended depth-of-field (eDOF). Recent advances in high-speed access to the axial dimension have made video-rate (>10 Hz) volumetric MPM progressively more practical.

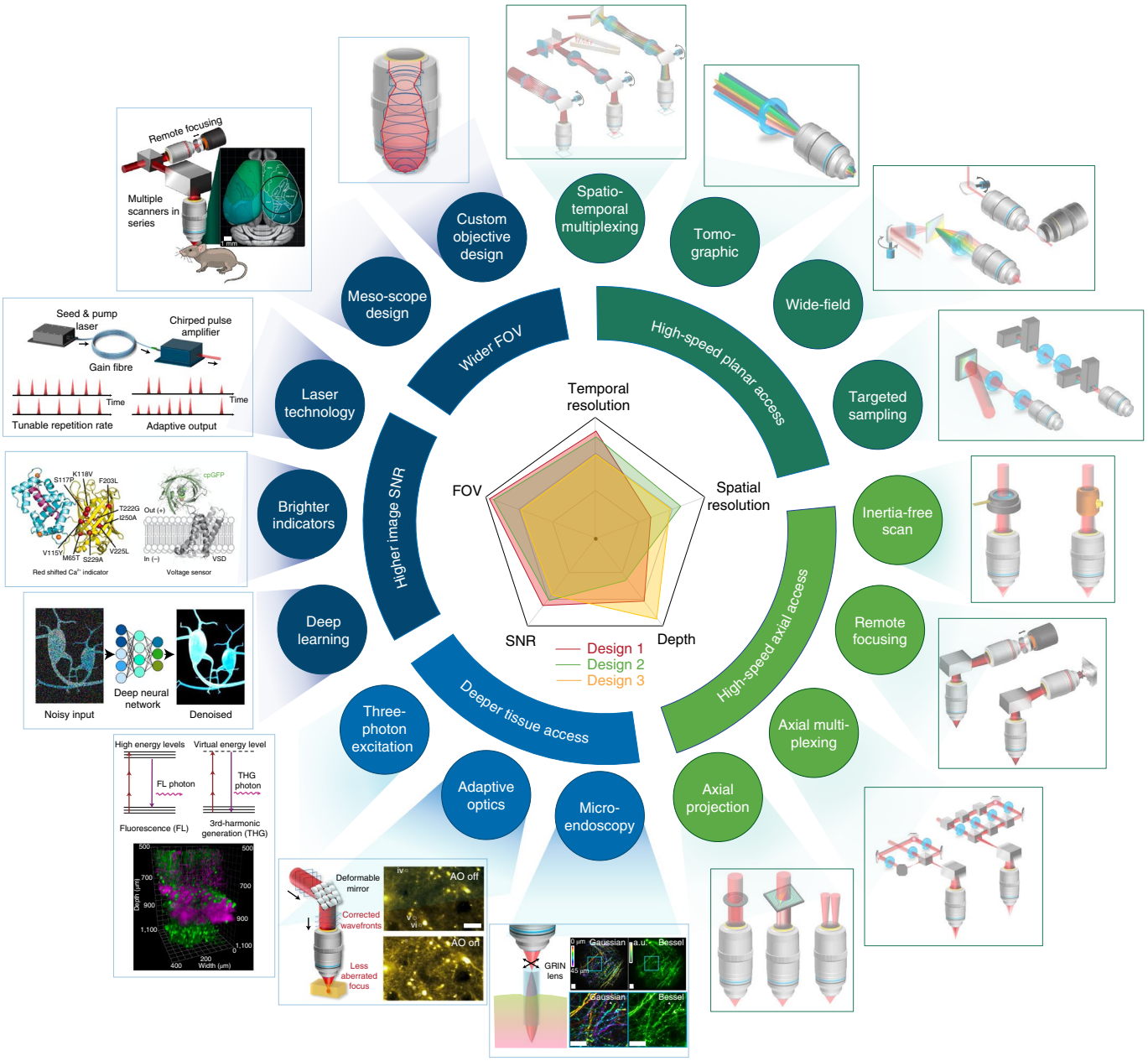

Fig. 4 | Ongoing advances in MPM that address the challenges of imaging a FOV, SNR and tissue penetration, together with temporal and spatial resolution. A new generation of (high-speed) MPM is expected to involve more synergisms between methods and advanced high-speed MPM toolboxes (described in Figs. 2 and 3) so as to maximize the spatial/temporal resolution, FOV, SNR and deep tissue access depend on the application requirements (for example, hypothetical designs 1, 2 and 3 as shown in the figure). Images reproduced with permission from ref. [47], under a Creative Commons license CC BY 4.0; ref. [35], Elsevier; refs. [82] and [84], Springer Nature America, Inc.; ref. [104], under a Creative Commons license CC BY 4.0; ref. [94], under a Creative Commons license CC BY 4.0.

Continuous volumetric sampling. In contrast to the mechanical objective scanning methods (Box 2), various inertia-free methods are now available to move the laser focus/foci axially, without the need for translating the objective or sample. One approach is to use focus-tunable lens[38] (for example, electrically tunable lens (ETL)[39] and tunable acoustic gradient-index (TAG) lens)[40,41] (Fig. 3a). Combining the TAG lens with resonant galvo-scanners, full-frame 2PFM of Ca^{2+} signals in the dendritic spines of neurons at a volume rate up to 56 Hz across $60 \times 3.75 \times 40\,\mu m^3$ can be achieved[40]. Such a TAG-lens approach can also be used for generating a 2D scanning light sheet within a millisecond in a two-photon SPIM system[42]. The focus tuning design in both ETL and TAG lens generally does not take into account the higher-order aberration. Hence, additional effort on wavefront shaping/engineering is necessary to ensure diffraction-limited focus during the fast axial scan[43,44].

Another method is remote focusing, which controls focal shifts via an additional remote objective and a scan mirror (typically mounted with a voice coil motor[45]) positioned at the conjugate plane of the sample. As this remote scan mirror is typically light-weight and thus of low inertia, the axial scan speed can be significantly scaled up (1 kHz) compared to the objective actuation[46] (Fig. 3b). Although slower than a TAG lens, remote focusing allows

the scan pattern to be more arbitrarily defined in 3D across a wider range of focal shift (hundreds of micrometres)[46,47] without extra optical aberrations. Taking advantage of the flexibility of manipulating the scan pattern in remote focusing, Chakraborty et al. recently showed that the lateral beam scan motion can be effectively transformed into axial scanning at 12 kHz in 2PFM[48]. Lateral beam scans (in 2D) have also been adopted in SPIM for full-frame 3D imaging owing to this orthogonal system configuration. As the 2D raster scan rate and the camera frame rate continue to advance (beyond kilohertz), full-frame 3D SPIM at video rate or beyond is, in principle, feasible[25,26], but is often compromised by the limited sensitivity of the camera (down to a few hertz)[14,22,25,49,50] and limited by the photon budget. When prior knowledge of the dynamics is available (for example, periodic contraction of a beating heart), one could digitally reconstruct the 3D motion pictures in two-photon SPIM up to 0.5 kHz through post-processing synchronization of the motion[24].

Discrete multiplane sampling. Spatiotemporal multiplexing can also be employed for multiplane imaging in MPM by splitting the excitation pulse trains into time-delayed beamlets (nanoseconds apart), which are then focused on different imaging depths (approximately four image planes (for example, ref. [51]); Fig. 3c). In this way, the MPM signals are less susceptible to contamination by light-scattering tissue because they can be registered to the specific image planes based on their arrival time at the detector[51–53]. Another approach for spatiotemporal multiplexing is the 'reverberation optical loop'[54], from which the laser pulse generates a sequence of subpulses focused at different depths. This method allows multiplane 2PFM (four planes) of neuronal Ca^{2+} dynamics in the mouse motor cortex and olfactory bulb at video rate (30 Hz). Notably, the decreasing power trend along the subpulses sequence (due to the cavity ring-down effect of the loop) could automatically balance the increasing scattering loss in deep tissue, and a similar fluorescence signal level can be obtained across all the image planes.

Projection sampling. Another strategy to scale up the volume rate of MPM is to exploit eDOF imaging to capture a 2D projected view of a volumetric structure (Fig. 3d). This is useful for imaging sparsely labelled structures with minimal structural overlap in their 2D projections (for example, in neuronal and vasculature imaging in brain volumes). This approach generates an axially elongated focus, which can simultaneously read out the MPM signals within an extended axial range, thus making the 2D scan rate equivalent to the volumetric rate. The axially elongated focus can, in principle, be generated in the form of a non-diffracting beam that maintains its intensity generally invariant during propagation[55]. Practical examples employed in MPM include the Bessel beam[56–58] and the Airy beam[59,60]. Notably, scanning Bessel foci has enabled high-speed volumetric 2PFM (~30–100 Hz) of neural activity in the mouse brain[56] and zebrafish larvae[57], as well as vascular dynamics of mouse brain[58]. Robust operation of Bessel-based (or Airy-based) MPM requires a greater average laser power than the standard configuration using a raster-scan Gaussian beam, as the power spreads to the side lobes of the Bessel and Airy beams, requiring attention to the potential unwanted background signal and leading to an extra thermal load on the sample. Note that, as well as the Bessel or Airy focus, which is continuous along the axial dimension, multiple axially separated foci generated with an SLM have also been adopted for 2PFM to simultaneously access different axial planes[61]. A different 2D projection approach is to raster-scan an elongated and stereoscopic V-shaped point spread function (PSF) in 2D, which effectively produces twin 2D projection images in which the spatial offset between the projections encodes the axial information in the volume[62] at a 2PFM volume rate of 30 Hz. For a more densely labelled structure with temporally sparse dynamical patterns (for example, Ca^{2+} transients), a signal demixing algorithm is necessary to combat the increased background[63].

Challenges and opportunities ahead

Biological dynamics cover 3D spatial scales spanning from single cells (micrometres) to the whole-organ level (millimetres), including local and long-range neuronal activities in the complex brain network[64]. High-throughput in vitro imaging assays are now undergoing a dramatic shift to the use of organoid models (other than 2D cell cultures), where 3D live characterization of intact organoids (as large as millimetres) is becoming increasingly critical for large-scale spatiotemporal studies of organogenesis[65,66]. The full potential of recent high-speed MPM developments could be exploited for these growing demands, but only when the imaging range in both lateral and axial dimensions can be maximized in deep tissue without severely compromising image quality and fidelity. Here, we highlight the fundamental challenges and how the aforementioned frontier of high-speed MPM could bring new promise in pushing such limits (Fig. 4).

Wider FOV. For a required spatial resolution (and thus NA), guided by the application, enlarging the imaging FOV (that is, maximizing the image information capacity[67]) generally requires large beam diameter and custom-designed optical elements, such as a larger objective and laser scanners with larger lenses to support a wide angular scan range[47,52,68,69] or custom multiscale lens designs to cover an ultra-large FOV[70]. The system complexity often scales with the imaging FOV, as more compound lens modules are required to correct or reprioritize the optical aberrations that blur/distort the large-FOV image and decrease the multiphoton excitation efficiency. It is also feasible to achieve large FOV in MPM by carefully choosing the combinations of off-the-shelf optics. It has been demonstrated that systematic optical invariant analysis of commercially available optics can be used as an effective design strategy for large-FOV (diameter of 7 mm) and high-resolution (<1.7-μm lateral resolution) raster-scan 2PFM[71], with the caveats of additional loss of SNR and extra aberrations introduced when combining multiple optical components. Another strategy for extending the effective FOV is to access multiple distant areas on demand, as fast as possible, for example by spatiotemporal multiplexing of multiple FOVs[47,52] or by designing a fast rotating micro-optic-based beam scanner in the post-objective space[72]. These large-FOV methods also demonstrate the importance of also using fast scanning methods (mostly resonant mirror scanners in these cases[47,52,72]) in scaling the imaging pixel rate up to tens to hundreds of megapixels per second (Fig. 1a). To maintain high volumetric imaging speed, emergent large-FOV MPM systems are expected to increasingly incorporate the aforementioned fast axial scanning methods based on a TAG lens, ETL and remote focusing (or equivalent) instead of the axial scan of a heavy-weight objective. Notably, a Bessel beam scanning module has been incorporated into a two-photon mesoscope for large-scale volumetric brain imaging at synaptic resolution (recording >9,000 neurons within ~3 mm^3 at 1 Hz; ref. [73]). On some occasions, high (diffraction-limited) resolution can be carefully compromised for large FOV at high speed. For example, one could use TF to engineer a large PSF (~ $5\times5\times10\,\mu m^3$) that is small enough to sample a neuronal soma and its activity. Further combined with remote focusing and signal extraction of partially overlapping neurons, this method could record the neural activity of ~12,000 neurons within a volume of $1\times1\times1.2\,mm^3$ and at a volume rate of ~17 Hz in awake mice[74].

Deeper penetration. The maximal imaging depth in MPM is fundamentally limited by light attenuation in the biological tissues, which is a combined effect of light absorption and scattering[75]. Although the excitation intensity can, in principle, be increased to

maintain a decent level of SNR and imaging speed in deep tissue, it introduces extra confounding factors, such as a higher thermal load and elevated out-of-focus background[76,77]. As scattering and absorption are wavelength-dependent, knowledge of the scattering/absorption spectra of the imaged sample and thus the operation (excitation) wavelength become key to achieving practical deep MPM. To this end, three-photon (3P) excitation is advantageous, in two key aspects, to overcome the depth limit: (1) its longer excitation wavelength (~1,300–1,700 nm or beyond), favouring reduced scattering, especially in deep tissue (>600 μm)[78] and (2) the higher-order nonlinearity of 3P excitation, allowing stronger excitation localization and reduced out-of-focus background when compared to 2P excitation[77]. 3P fluorescence microscopy (3PFM) for practical deep tissue imaging has not been well conceived until very recently, thanks, in particular, to the advance in high-power femtosecond laser technology (for example, ref. [79]) and rapid progress in redshifted genetically encoded fluorescence indicators[80–82]. The majority of the latest 3PFM systems have been particularly successful in in vivo deep brain imaging (>500 μm), but generally at a modest 2D frame rate (~10 f.p.s.)[74,76,83–85]. To maximize the imaging rate of 3PFM, one could leverage the established high-speed imaging strategies used for 2PFM, many of which are compatible with 3PFM. Examples include 3PFM with remote focusing and spatiotemporal multiplexing[74,86]. This combined approach allows a 3PFM volume rate of 3.9 Hz ($340 \times 340 \times 250\,\mu m^3$) at ~1-mm depth through the intact cortex of the mouse brain[74]. Furthermore, parallelization in 3PFM is, in principle, feasible, but with special attention to the high illumination power (~260 mW)[87]. Restricting the parallelization to 1D thus appears more favourable for live imaging. Bessel beam excitation, using ~30–100 mW, allows 3PFM in vivo mouse brain imaging at a volumetric rate of 1 Hz, at ~100–600 μm below the dura[88,89].

To perform high-resolution live imaging beyond a few millimetres deep in biological tissue, the only viable approach so far has been to implant the microendoscopic optical assembly (for example, microprisms[90] and gradient refractive index (GRIN) lenses[91,92]) into the deep tissue region of interest based on minimally invasive stereotactic surgical protocols[93]. Careful optical design allows incorporation of many of the aforementioned high-speed scanning methods in the microendoscopic system, such that the high-speed scanning foci can be relayed through the GRIN lens with minimal aberration, for example, Bessel focus scanning[94], targeted sampling using patterned illumination[95] and multiplane random-access sampling using ETL[96,97]. The fast axial scan (tens of kilohertz) offered by a TAG lens can also be implemented with two-photon microendoscopy to achieve an ~4-Hz volume rate[98]. To achieve high-quality microendoscopy, the intrinsic aberration of GRIN lenses can be corrected by either a custom-designed compound GRIN lens module (for example, including aspheric microlenses[99]) or adaptive optics (AO)[100,101].

Originally applied in astronomical telescopes, the AO methods applied in microscopy generally measure (direct and indirect sensing) and correct the wavefront distortion of the excitation light introduced by the tissue inhomogeneity and optical aberration induced by the system, and thus restore nearly diffraction-limited resolution. Details of the different AO methods are described in refs. [102,103]. Generally, direct sensing methods[104–106] are faster (<1 s to correct the wavefront), but they only work well with weakly scattered tissue (for example, functional retinal imaging in vivo[106]). On the other hand, indirect sensing[100,107,108] is well suited for highly scattered tissue at the expense of aberration-correction speed (taking seconds to minutes for aberration measurement). Recently, an indirect sensing approach based on frequency multiplexing was demonstrated to enable a 4× speed improvement over its previous generation and could also be applicable to both 2PFM and 3PFM[109].

Better SNR. Going hand in hand with the strategies for increasing the MPM imaging speed, the development of new high-energy pulsed laser sources, the heart of all MPM systems, is a foundational approach to maximize the photon budget. In general, lowering the laser repetition rate and increasing the pulse peak intensity (that is, keeping the average power constant) can effectively enhance the MPM signal and reduce heating-induced tissue damage[24,77,110], but with the risk of increased nonlinear photodamage and photobleaching[111]. As the interplay between (linear) photothermal damage and higher-order nonlinear photodamage/photobleaching remains unclear and is likely to be highly problem-specific (for example, imaging conditions and the choices of fluorophore), an adjustable repetition rate is a practical attribute for adapting to the different imaging/sample conditions and thus achieving the best optimal imaging performance (with maximally permissible MPM signal) (for example, ref. [24] for 2P-SPIM and ref. [78] for 3PFM). Notably, the rapid progress in solid-state lasers[112] and rare-earth-doped fibre lasers[113–115] has led to versatile solutions for low-repetition-rate (one to tens of megahertz) ultrashort pulses (~100–200 fs). As well as a tunable repetition rate, scalable power tuning is also achievable, which is essential for high-speed imaging based on multifoci or spatiotemporally multiplexed illumination patterns (sub-microjoules[74]) and wider wavelength accessibility (1,000–1,700 nm)[79]. The flexibility of fibre lasers has recently been taken to a new level where the laser pulses can be adaptively generated to illuminate a region of interest to maximize the photon budget in both 2PFM and 3PFM[116]. As far as speed scaling is concerned, one can accelerate the imaging pixel rate by increasing the laser repetition rate (maintaining the original pulse intensity is required). However, the signal read out from each pixel requires averaging multiple laser pulses in favour of a better SNR. Hence, the reported pixel rate of conventional MPM systems (especially beyond five years ago) is generally well below 1–10 Mpixel s^{-1} (Fig. 1a). For a given laser repetition rate, the room for averaging could be limited to maintain a high imaging speed, especially when the 2D frame rate is required to reach the kilohertz regime. In this scenario, a laser design with high pulse-to-pulse temporal stability (better to be less than a few percent[117]) and low timing jitter also becomes increasingly critical to ensure low-noise imaging at high speed. Progress in both laser technologies and imaging techniques will also continue to spur the development of new fluorescent probes that could favour efficient longer-wavelength multiphoton excitation (for example, redshifted genetically encoded calcium indicators[118,119]; most importantly, it allows robust and bright fluorescence emission at high speed (for example, genetically encoded voltage indicator (ASAP3)[35])—all favouring better imaging sensitivity.

Image restoration or denoising by computational methods is another strategy to combat image SNR degradation at high speed (because of shorter exposure times) and under the common low-light condition found in MPM. In recent years, deep learning, especially with convolutional neural networks, has shown impressive denoising performance, superior to the classical denoising algorithms[120]. For example, by training the convolutional neural networks with low- and high-SNR image pairs, a content-aware image restoration (CARE) method can effectively denoise the fluorescence images, even when the light exposure is reduced by 60 times[121]. Apart from using the matched pairs of training images (which are not always available), self-supervised learning approaches[122] and generative models (cycleGAN)[123] have recently shown promise in denoising and can readily be applied to MPM imaging problems. Readers can refer to recent reviews[124,125] for more details regarding the latest developments of deep learning augmenting the performance of optical microscopy.

Concluding remarks

To push the limit of the overall imaging performance at high speed (that is, wider FOV and/or deeper penetration with high

image fidelity), new-generation MPM is expected, in the near future, to involve reinvention of the existing high-speed strategies described above in different combinations. This will inevitably increase the complexity of the instrumentation, which will require specialized (and costly) technical expertise and impede the accessibility to advanced microscopes for the wider biological community. Hence, ongoing development should pay more attention to the issues of 'how easily can the new MPM techniques reach the hands of biologists?' and 'how straightforwardly can the new high-speed strategies be adapted to (and thus transform) existing MPM systems?'.

One barrier is the use of high-power Ti:sapphire lasers or parametric oscillators in the MPM system that are bulky (~10 m^2), costly (US$200,000 or more) and require frequent maintenance. The emergent high-power fibre lasers, as well as mode-locked semiconductor lasers[126], are promising alternatives to traditional light sources, offering equivalent or even better MPM imaging performance with cost-effective, compact and turnkey operation. Equally challenging is the backend support for managing high-speed data acquisition, processing and storage. For example, a state-of-the-art high-bandwidth digitizer is essential to support 2D kilohertz MPM, which could require an image pixel rate of hundreds of megapixels per second or more (Fig. 1a). For continuous image recording, traditional offline image processing (reconstruction, denoising, segmentation and so on) will become an increasingly daunting task due to the sheer amount of raw data. Hence, there is a pressing need for improved capability for real-time, in situ high-performance data processing (for example, using a field-programmable gate array and/or graphic processing unit) as data are generated from the imaging front end. However, successful deployment of these computational procedures (for example, distributing real-time computation steps in hardware with pipeline parallelism) requires expert knowledge in hardware computation design and engineering, which might not be readily available in many biological research laboratories.

Wider dissemination requires a cohesive community of MPM developers that can promote collective initiatives in offering open-access resources, including laser design, imaging instrument hardware, imaging protocols, sample preparation and image-processing pipelines (for example, several SPIM open-source projects[127]). Given that the increasingly diverse high-speed methods are implemented as an add-on to standard MPM systems (for example, modules of ultrafast laser scanning, remote focusing and random access), repertoires of modularized options could be provided in the open-access platform for developers to custom their MPM system according to their target applications[128]. This requires coordinated effort within a home-building community that will make different technical specifications translatable and compatible between different laboratories, promote image data standardization and interoperability, and ultimately ensure full system customizability. It is equally critical to establish a more intensified scientific synergism between microscope developers and biologists than ever. This collaboration will ensure that advanced MPM systems will be tailored and refined to tackle well-defined biological problems, enabling innovative development and tangible discoveries to proceed in parallel (for example, the Allen Institute's OpenScope project). Overall, the recent breakthroughs in scaling MPM speed have created diverse possibilities to break the status quo of this three-decade-old technology, and, while continuing to fuel the intense interest in studying fast dynamical neuronal activities, they could also drive explorations of new applications in other areas, notably high-throughput image-based screening using MPM.

Received: 21 March 2021; Accepted: 19 August 2021;
Published online: 27 October 2021

References

1. Hooke, R. *Micrographia: or Some Physiological Descriptions of Minute Bodies Made by Magnifying Glasses. With Observations and Inquiries Thereupon* (The Royal Society, 1665).
2. Denk, W., Strickler, J. H. & Webb, W. W. Two-photon laser scanning fluorescence microscopy. *Science* **248**, 73–76 (1990).
3. Göppert-Mayer, M. Über Elementarakte mit zwei Quantensprüngen. *Ann. Phys.* **9**, 273–294 (1931).
4. Bahlmann, K. et al. Multifocal multiphoton microscopy (MMM) at a frame rate beyond 600 Hz. *Opt. Express* **15**, 10991–10998 (2007).
5. Zhang, T. et al. Kilohertz two-photon brain imaging in awake mice. *Nat. Methods* **16**, 1119–1122 (2019).
6. Sacconi, L. et al. Multiphoton multifocal microscopy exploiting a diffractive optical element. *Opt. Lett.* **28**, 1918–1920 (2003).
7. Nikolenko, V. et al. SLM microscopy: scanless two-photon imaging and photostimulation with spatial light modulators. *Front. Neural Circuits* **2**, 5 (2008).
8. Wu, J. et al. Kilohertz two-photon fluorescence microscopy imaging of neural activity in vivo. *Nat. Methods* **17**, 287–290 (2020).
9. Wu, J. et al. Ultrafast laser-scanning time-stretch imaging at visible wavelengths. *Light Sci. Appl.* **6**, e16196 (2017).
10. Karpf, S. et al. Spectro-temporal encoded multiphoton microscopy and fluorescence lifetime imaging at kilohertz frame-rates. *Nat. Commun.* **11**, 2062 (2020).
11. Mandracchia, B. et al. Fast and accurate sCMOS noise correction for fluorescence microscopy. *Nat. Commun.* **11**, 94 (2020).
12. Voleti, V. et al. Real-time volumetric microscopy of in vivo dynamics and large-scale samples with SCAPE 2.0. *Nat. Methods* **16**, 1054–1062 (2019).
13. Schrödel, T., Prevedel, R., Aumayr, K., Zimmer, M. & Vaziri, A. Brain-wide 3D imaging of neuronal activity in *Caenorhabditis elegans* with sculpted light. *Nat. Methods* **10**, 1013–1020 (2013).
14. Truong, T. et al. Deep and fast live imaging with two-photon scanned light-sheet microscopy. *Nat. Methods* **8**, 757–760 (2011).
15. Oron, D., Tal, E. & Silberberg, Y. Scanningless depth-resolved microscopy. *Opt. Express* **13**, 1468–1476 (2005).
16. Zhu, G., Van Howe, J., Durst, M., Zipfel, W. & Xu, C. Simultaneous spatial and temporal focusing of femtosecond pulses. *Opt. Express* **13**, 2153–2159 (2005).
17. Papagiakoumou, E., Ronzitti, E. & Emiliani, V. Scanless two-photon excitation with temporal focusing. *Nat. Methods* **17**, 571–581 (2020).
18. Podgorski, K. & Ranganathan, G. Brain heating induced by nearinfrared lasers during multiphoton microscopy. *J. Neurophysiol.* **116**, 1012–1023 (2016).
19. Dana, H. et al. Hybrid multiphoton volumetric functional imaging of large-scale bioengineered neuronal networks. *Nat. Commun.* **5**, 3997 (2014).
20. Xue, Y. et al. Scanless volumetric imaging by selective access multifocal multiphoton microscopy. *Optica* **6**, 76–83 (2019).
21. Hillman, E. M. C., Voleti, V., Li, W. & Yu, H. Light-sheet microscopy in neuroscience. *Annu. Rev. Neurosci.* **42**, 295–313 (2019).
22. Wolf, S. et al. Whole-brain functional imaging with two-photon light-sheet microscopy. *Nat. Methods* **12**, 379–380 (2015).
23. Mahou, P., Vermot, J., Beaurepaire, E. & Supatto, W. Multicolor two-photon light-sheet microscopy. *Nat. Methods* **11**, 600–601 (2014).
24. Maioli, V. et al. Fast in vivo multiphoton light-sheet microscopy with optimal pulse frequency. *Biomed. Opt. Express* **11**, 6012–6026 (2020).
25. Kumar, M. et al. Integrated one- and two-photon scanned oblique plane illumination (SOPi) microscopy for rapid volumetric imaging. *Opt. Express* **26**, 13027–13041 (2018).
26. Sapoznik, E. et al. A versatile oblique plane microscope for large-scale and high-resolution imaging of subcellular dynamics. *eLife* **9**, e57681 (2020).
27. Kazemipour, A. et al. Kilohertz frame-rate two-photon tomography. *Nat. Methods* **16**, 778–786 (2019).
28. Escobet-Montalbán, A. et al. Wide-field multiphoton imaging through scattering media without correction. *Sci. Adv.* **4**, eaau1338 (2018).
29. Katona, G. et al. Fast two-photon in vivo imaging with three-dimensional random-access scanning in large tissue volumes. *Nat. Methods* **9**, 201–208 (2012).
30. Sakaki, K. D. R., Podgorski, K., Toth, T. A. D., Coleman, P. & Haas, K. Comprehensive imaging of sensory-evoked activity of entire neurons within the awake developing brain using ultrafast AOD-based random-access two-photon microscopy. *Front. Neural Circuits* **14**, 33 (2020).
31. Nadella, K. M. et al. Random-access scanning microscopy for 3D imaging in awake behaving animals. *Nat. Methods* **13**, 1001–1004 (2016).
32. Szalay, G. et al. Fast 3D imaging of spine, dendritic and neuronal assemblies in behaving animals. *Neuron* **92**, 723–738 (2016).
33. Li, B. et al. Two-photon voltage imaging of spontaneous activity from multiple neurons reveals network activity in brain tissue. *iScience* **23**, 101363 (2020).

34. Chamberland, S. et al. Fast two-photon imaging of subcellular voltage dynamics in neuronal tissue with genetically encoded indicators. *eLife* **6**, e25690 (2017).
35. Villette, V. et al. Ultrafast two-photon imaging of a high-gain voltage indicator in awake behaving mice. *Cell* **179**, 1590–1608 (2019).
36. Geng, Q., Gu, C., Cheng, J. & Chen, S.-H. Digital micromirror device-based two-photon microscopy for three-dimensional and random-access imaging. *Optica* **4**, 674–677 (2017).
37. Griffiths, V. A. et al. Real-time 3D movement correction for two-photon imaging in behaving animals. *Nat. Methods* **17**, 741–748 (2020).
38. Kang, S., Duocastella, M. & Arnold, C. B. Variable optical elements for fast focus control. *Nat. Photon.* **14**, 533–542 (2020).
39. Grewe, B. F., Voigt, F. F., van't Hoff, M. & Helmchen, F. Fast two-layer two-photon imaging of neuronal cell populations using an electrically tunable lens. *Biomed. Opt. Express* **2**, 2035–2046 (2011).
40. Kong, L. et al. Continuous volumetric imaging via an optical phase-locked ultrasound lens. *Nat. Methods* **12**, 759–762 (2015).
41. Piazza, S., Bianchini, P., Sheppard, C., Diaspro, A. & Duocastella, M. Enhanced volumetric imaging in 2-photon microscopy via acoustic lens beam shaping. *J. Biophoton.* **11**, e201700050 (2018).
42. Zong, W. et al. Large-field high-resolution two-photon digital scanned light-sheet microscopy. *Cell Res.* **25**, 254–257 (2015).
43. Žurauskas, M., Barnstedt, O., Frade-Rodriguez, M., Waddell, S. & Booth, M. J. Rapid adaptive remote focusing microscope for sensing of volumetric neural activity. *Biomed. Opt. Express* **8**, 4369–4379 (2017).
44. Peinado, A., Bendek, E., Yokoyama, S. & Poskanzer, K. E. Deformable mirror-based axial scanning for two-photon mammalian brain imaging. *Neurophotonics* **8**, 015003 (2021).
45. Rupprecht, P., Prendergast, A., Wyart, C. & Friedrich, R. W. Remote *z*-scanning with a macroscopic voice coil motor for fast 3D multiphoton laser scanning microscopy. *Biomed. Opt. Express* **7**, 1656–1671 (2016).
46. Botcherby, E. J. et al. Aberration-free three-dimensional multiphoton imaging of neuronal activity at kHz rates. *Proc. Natl Acad. Sci. USA* **109**, 2919–2924 (2012).
47. Sofroniew, N. J., Flickinger, D., King, J. & Svoboda, K. A large field of view two-photon mesoscope with subcellular resolution for in vivo imaging. *eLife* **5**, e14472 (2016).
48. Chakraborty, T. et al. Converting lateral scanning into axial focusing to speed up three-dimensional microscopy. *Light Sci. Appl.* **9**, 165 (2020).
49. Planchon, T. et al. Rapid three-dimensional isotropic imaging of living cells using Bessel beam plane illumination. *Nat. Methods* **8**, 417–423 (2011).
50. Shin, Y., Kim, D. & Kwon, H.-S. Oblique scanning 2-photon light-sheet fluorescence microscopy for rapid volumetric imaging. *J. Biophoton.* **11**, e201700270 (2017).
51. Cheng, A., Gonçalves, J. T., Golshani, P., Arisaka, K. & Portera-Cailliau, C. Simultaneous two-photon calcium imaging at different depths with spatiotemporal multiplexing. *Nat. Methods* **8**, 139–142 (2011).
52. Stirman, J. N., Smith, I. T., Kudenov, M. W. & Smith, S. L. Wide field-of-view, multi-region, two-photon imaging of neuronal activity in the mammalian brain. *Nat. Biotechnol.* **34**, 857–862 (2016).
53. Chen, J. L., Voigt, F. F., Javadzadeh, M., Krueppel, R. & Helmchen, F. Long-range population dynamics of anatomically defined neocortical networks. *eLife* **5**, e14679 (2016).
54. Beaulieu, D. R. et al. Simultaneous multiplane imaging with reverberation two-photon microscopy. *Nat. Methods* **17**, 283–286 (2020).
55. Durnin, J., Miceli, J. J. & Eberly, J. H. Diffraction-free beams. *Phys. Rev. Lett.* **58**, 1499–1501 (1987).
56. Lu, R. et al. Video-rate volumetric functional imaging of the brain at synaptic resolution. *Nat. Neurosci.* **20**, 620–628 (2017).
57. Lu, R., Tanimoto, M., Koyama, M. & Ji, N. 50-Hz volumetric functional imaging with continuously adjustable depth of focus. *Biomed. Opt. Express* **9**, 1964–1976 (2018).
58. Fan, J. L. et al. High-speed volumetric two-photon fluorescence imaging of neurovascular dynamics. *Nat. Commun.* **11**, 6020 (2020).
59. Tan, X. J. et al. Volumetric two-photon microscopy with a non-diffracting Airy beam. *Opt. Lett.* **44**, 391–394 (2019).
60. He, H. et al. Depth-resolved volumetric two-photon microscopy based on dual Airy beam scanning. *Opt. Lett.* **44**, 5238–5241 (2019).
61. Yang, W. et al. Simultaneous multi-plane imaging of neural circuits. *Neuron* **20**, 269–284 (2016).
62. Song, A. et al. Volumetric two-photon imaging of neurons using stereoscopy (vTwINS). *Nat. Methods* **14**, 420–426 (2017).
63. Pnevmatikakis, E. A. et al. Simultaneous denoising, deconvolution and demixing of calcium imaging data. *Neuron* **89**, 285–299 (2016).
64. Oh, S. W. et al. A mesoscale connectome of the mouse brain. *Nature* **508**, 207–214 (2014).
65. Dekkers, J. F. et al. High-resolution 3D imaging of fixed and cleared organoids. *Nat. Protoc.* **14**, 1756–1771 (2019).
66. Weeber, F., Ooft, S. N., Dijkstra, K. K. & Voest, E. E. Tumor organoids as a pre-clinical cancer model for drug discovery. *Cell Chem. Biol.* **24**, 1092–1100 (2019).
67. Lohmann, A. W., Dorsch, R. G., Mendlovic, D., Zalevsky, Z. & Ferreira, C. Space–bandwidth product of optical signals and systems. *J. Opt. Soc. Am. A* **13**, 470–473 (1996).
68. McConnell, G. et al. A novel optical microscope for imaging large embryos and tissue volumes with sub-cellular resolution throughout. *eLife* **5**, e18659 (2016).
69. Tsai, P. S. et al. Ultra-large field-of-view two-photon microscopy. *Opt. Express* **23**, 13833–13847 (2015).
70. Fan, J. et al. Video-rate imaging of biological dynamics at centimetre scale and micrometre resolution. *Nat. Photon.* **13**, 809–816 (2019).
71. Bumstead, J. R. et al. Designing a large field-of-view two-photon microscope using optical invariant analysis. *Neurophotonics* **5**, 025001 (2018).
72. Terada, S. I., Kobayashi, K., Ohkura, M., Nakai, J. & Matsuzaki, M. Superwide-field two-photon imaging with a micro-optical device moving in post-objective space. *Nat. Commun.* **9**, 3550 (2018).
73. Lu, R. et al. Rapid mesoscale volumetric imaging of neural activity with synaptic resolution. *Nat. Methods* **17**, 291–294 (2020).
74. Weisenburger, S. et al. Volumetric Ca^{2+} imaging in the mouse brain using hybrid multiplexed sculpted light microscopy. *Cell* **177**, 1050–1066 (2019).
75. Tsia, K. (ed.) *Understanding Biophotonics*: *Fundamentals*, *Advances and Applications* (CRC Press, 2016).
76. Horton, N. G. et al. In vivo three-photon microscopy of subcortical structures within an intact mouse brain. *Nat. Photon.* **7**, 205–209 (2013).
77. Wang, T. & Xu, C. Three-photon neuronal imaging in deep mouse brain. *Optica* **7**, 947–960 (2020).
78. Wang, T. et al. Quantitative analysis of 1,300-nm three-photon calcium imaging in the mouse brain. *eLife* **9**, e53205 (2020).
79. Guesmi, K. et al. Dual-color deep-tissue three-photon microscopy with a multiband infrared laser. *Light Sci. Appl.* **7**, 12 (2018).
80. Dana, H. et al. Sensitive red protein calcium indicators for imaging neural activity. *eLife* **5**, e12727 (2016).
81. Kannan, M. et al. Fast, in vivo voltage imaging using a red fluorescent indicator. *Nat. Methods* **15**, 1108–1116 (2018).
82. Mohr, M. A. et al. jYCaMP: an optimized calcium indicator for two-photon imaging at fiber laser wavelengths. *Nat. Methods* **17**, 694–697 (2020).
83. Yildirim, M., Sugihara, H., So, P. T. & Sur, M. Functional imaging of visual cortical layers and subplate in awake mice with optimized three-photon microscopy. *Nat. Commun.* **10**, 177 (2019).
84. Ouzounov, D. G. et al. In vivo three-photon imaging of activity of GCaMP6-labeled neurons deep in intact mouse brain. *Nat. Methods* **14**, 388–390 (2017).
85. Wang, T. et al. Three-photon imaging of mouse brain structure and function through the intact skull. *Nat. Methods* **15**, 789–792 (2018).
86. Takasaki, K. T., Tsyboulski, D. & Waters, J. Dual-plane 3-photon microscopy with remote focusing. *Biomed. Opt. Express* **10**, 5585–5599 (2019).
87. Escobet-Montalbán, A. et al. Three-photon light-sheet fluorescence microscopy. *Opt. Lett.* **43**, 5484–5487 (2018).
88. Rodríguez, C., Liang, Y., Lu, R. & Na, J. Three-photon fluorescence microscopy with an axially elongated Bessel focus. *Opt. Lett.* **43**, 1914–1917 (2018).
89. Chen, B. et al. Rapid volumetric imaging with Bessel-beam three-photon microscopy. *Biomed. Opt. Express* **9**, 1992–2000 (2018).
90. Low, R. J., Gu, Y. & Tank, D. W. Cellular resolution optical access to brain regions in fissures: imaging medial prefrontal cortex and grid cells in entorhinal cortex. *Proc. Natl Acad. Sci. USA* **111**, 18739–18744 (2014).
91. Ozbay, B. N. et al. Three dimensional two-photon brain imaging in freely moving mice using a miniature fiber coupled microscope with active axial-scanning. *Sci. Rep.* **8**, 8108 (2018).
92. Attardo, A., Fitzgerald, J. E. & Schnitzer, M. J. Impermanence of dendritic spines in live adult CA1 hippocampus. *Nature* **523**, 592–596 (2015).
93. Liang, B., Zhang, L., Moffitt, C., Li, Y. & Lin, D. T. An open-source automated surgical instrument for microendoscope implantation. *J. Neurosci. Methods* **311**, 83–88 (2019).
94. Meng, G. et al. High-throughput synapse-resolving two-photon fluorescence microendoscopy for deep-brain volumetric imaging in vivo. *eLife* **8**, e40805 (2019).
95. Moretti, C., Antonini, A., Bovetti, S., Liberale, C. & Fellin, T. Scanless functional imaging of hippocampal networks using patterned two-photon illumination through GRIN lenses. *Biomed. Opt. Express* **7**, 3958–3967 (2016).
96. Sato, M. et al. Fast varifocal two-photon microendoscope for imaging neuronal activity in the deep brain. *Biomed. Opt. Express* **8**, 4049–4060 (2017).

97. Qin, Z. et al. Adaptive optics two-photon endomicroscopy enables deep-brain imaging at synaptic resolution over large volumes. *Sci. Adv.* **6**, eabc6521 (2020).
98. Chien, Y. F. et al. Dual GRIN lens two-photon endoscopy for high-speed volumetric and deep brain imaging. *Biomed. Opt. Express* **12**, 162–172 (2021).
99. Antonini, A. et al. Extended field-of-view ultrathin microendoscopes for high-resolution two-photon imaging with minimal invasiveness. *eLife* **9**, e58882 (2020).
100. Wang, C. & Ji, N. Characterization and improvement of three-dimensional imaging performance of GRIN-lens-based two-photon fluorescence endomicroscopes with adaptive optics. *Opt. Express* **21**, 27142–27154 (2013).
101. Wang, C. & Ji, N. Pupil-segmentation-based adaptive optical correction of a high-numerical-aperture gradient refractive index lens for two-photon fluorescence endoscopy. *Opt. Lett.* **37**, 2001–2003 (2012).
102. Ji, N. Adaptive optical fluorescence microscopy. *Nat. Methods* **14**, 374–380 (2017).
103. Booth, M. Adaptive optical microscopy: the ongoing quest for a perfect image. *Light Sci. Appl.* **3**, e165 (2014).
104. Wang, K. et al. Direct wavefront sensing for high-resolution in vivo imaging in scattering tissue. *Nat. Commun.* **6**, 7276 (2015).
105. Liu, R., Li, Z., Marvin, J. S. & Kleinfeld, D. Direct wavefront sensing enables functional imaging of infragranular axons and spines. *Nat. Methods* **16**, 615–618 (2019).
106. Qin, Z. et al. Adaptive optics two-photon microscopy enables near-diffraction-limited and functional retinal imaging in vivo. *Light Sci. Appl.* **9**, 79 (2020).
107. Ji, N., Milkie, D. E. & Betzig, E. Adaptive optics via pupil segmentation for high-resolution imaging in biological tissues. *Nat. Methods* **7**, 141–147 (2010).
108. Park, J. H., Kong, L., Zhou, Y. & Cui, M. Large-field-of-view imaging by multi-pupil adaptive optics. *Nat. Methods* **14**, 581–583 (2017).
109. Rodríguez, C. et al. An adaptive optics module for deep tissue multiphoton imaging in vivo. Preprint at *bioRxiv* https://doi.org/10.1101/2020.11.25.397968 (2020).
110. Charan, K., Li, B., Wang, M., Lin, C. P. & Xu, C. Fiber-based tunable repetition rate source for deep tissue two-photon fluorescence microscopy. *Biomed. Opt. Express* **9**, 2304–2311 (2018).
111. Ji, N., Magee, J. C. & Betzig, E. High-speed, low-photodamage nonlinear imaging using passive pulse splitters. *Nat. Methods* **5**, 197–202 (2008).
112. Perillo, E. et al. Two-color multiphoton in vivo imaging with a femtosecond diamond Raman laser. *Light Sci. Appl.* **6**, e17095 (2017).
113. Perillo, E. P. et al. Deep in vivo two-photon microscopy with a low cost custom built mode-locked 1,060-nm fiber laser. *Biomed. Opt. Express* **7**, 324–334 (2016).
114. Chen, B. et al. Robust hollow-fiber-pigtailed 930-nm femtosecond Nd:fiber laser for volumetric two-photon imaging. *Opt. Express* **25**, 22704–22709 (2017).
115. Stachowiak, D. et al. Frequency-doubled femtosecond Er-doped fiber laser for two-photon excited fluorescence imaging. *Biomed. Opt. Express* **11**, 4431–4442 (2020).
116. Li, B., Wu, C., Wang, M., Charan, K. & Xu, C. An adaptive excitation source for high-speed multiphoton microscopy. *Nat. Methods* **17**, 163–167 (2020).
117. Kong, C. et al. High-contrast, fast chemical imaging by coherent Raman scattering using a self-synchronized two-colour fibre laser. *Light Sci. Appl.* **9**, 25 (2020).
118. Qian, Y. et al. A genetically encoded near-infrared fluorescent calcium ion indicator. *Nat. Methods* **16**, 171–174 (2019).
119. Shemetov, A. A. et al. A near-infrared genetically encoded calcium indicator for in vivo imaging. *Nat. Biotechnol.* **39**, 368–377 (2021).
120. Zhang, K., Zuo, W., Chen, Y., Meng, D. & Zhang, L. Beyond a Gaussian denoiser: residual learning of deep CNN for image denoising. *IEEE Trans. Image Process.* **26**, 3142–3155 (2017).
121. Weigert, M. et al. Content-aware image restoration: pushing the limits of fluorescence microscopy. *Nat. Methods* **15**, 1090–1097 (2018).
122. Batson, J. & Royer, L. Noise2Self: blind denoising by self-supervision. *Proc. 36th International Conference on Machine Learning (PMLR)* **97**, 524–533 (2019).
123. Zhu, J., Park, T., Isola, P. & Efros, A. A. Unpaired image-to-image translation using cycle-consistent adversarial networks. In *Proc. 2017 IEEE International Conference on Computer Vision (ICCV)* 2242–2251 (IEEE, 2017).
124. Moen, E. et al. Deep learning for cellular image analysis. *Nat. Methods* **16**, 1233–1246 (2019).
125. Belthangady, C. & Royer, L. A. Applications, promises and pitfalls of deep learning for fluorescence image reconstruction. *Nat. Methods* **16**, 1215–1225 (2019).
126. Voigt, F. F. et al. Multiphoton in vivo imaging with a femtosecond semiconductor disk laser. *Biomed. Opt. Express* **8**, 3213–3231 (2017).
127. Pitrone, P. G. et al. OpenSPIM: an open-access light-sheet microscopy platform. *Nat. Methods* **10**, 598–599 (2013).
128. Pachitariu, M. et al. Suite2p: beyond 10,000 neurons with standard two-photon microscopy. Preprint at *bioRxiv* https://doi.org/10.1101/061507 (2017).
129. Marshall, G. F. & Stutz, G. E. (eds) *Handbook of Optical and Laser Scanning* (Taylor & Francis, 2012).
130. Grewe, B. F., Langer, D., Kasper, H., Kampa, B. M. & Helmchen, F. High-speed in vivo calcium imaging reveals neuronal network activity with near-millisecond precision. *Nat. Methods* **7**, 399–405 (2010).
131. Cossell, L. et al. Functional organization of excitatory synaptic strength in primary visual cortex. *Nature* **518**, 399–403 (2015).
132. Katona, G. et al. Roller coaster scanning reveals spontaneous triggering of dendritic spikes in CA1 interneurons. *Proc. Natl Acad. Sci. USA* **108**, 2148–2153 (2011).

Acknowledgements

This work is supported by the Research Grants Council of the Hong Kong Special Administrative Region of China (grants 17208918, 17209017 and 17259316 to J.W. and K.K.T.; RFS2021-7S06 and C7047-16G to K.K.T.) and NIH BRAIN Initiative grants (1UF1NS107696 to J.W., N.J. and K.K.T.).

Author contributions

All authors contributed to writing the manuscript.

Competing interests

The authors declare no competing interests.

Additional information

Supplementary information The online version contains supplementary material available at https://doi.org/10.1038/s41566-021-00881-0.

Correspondence should be addressed to Na Ji or Kevin K. Tsia.

Peer review information *Nature Photonics* thanks Keisuke Goda and the other, anonymous, reviewer(s) for their contribution to the peer review of this work.